19th Australasian Fluid Mechanics Conference
Melbourne, Australia
8-11 December 2014

Particle Collection Using Vibrating Bubbles

H.V. Phan, M. Şeşen, T. Alan and A. Neild

Department of Mechanical and Aerospace Engineering
Monash University, Melbourne 3800, Australia

Abstract

In this study, we present a microfluidics channel capable of collecting and focusing particles by the use of a vibrating air/water interface. The device contains a sidewall cylindrical void that traps air to create a microbubble surface, a modified version of the commonly used lateral cavity acoustic transducer (LCAT). By employing a relatively narrow rectangular channel (50 μm wide), we show that particles can be trapped and released into a narrow region. The collection process is described through an analysis of the transient state of the vortex. Additionally, it is found that the focusing efficiency, i.e. the width of focusing region, depends on the particles diameter and the excitation amplitude. 6.60 μm particles can easily be made to form a single line along the channel wall opposite the bubble under suitable conditions. For 2.01 μm particles, the focussing can be to a region of one third of the channel width. The focusing width grows with decreasing excitation amplitude, down to a certain voltage beyond which the vortices are too weak to induce any streaming.

Introduction

Microfluidics platforms, or lab-on-a-chip (LOC) devices, are becoming increasingly important in many fields of life sciences, such as chemical analysis [10, 19] and molecular biology [20, 32]. There are many phenomena that are exclusive to microfluidic channel, all of which can be categorised into two groups: passive and active method. A particularly versatile design is an acoustically excited air-water microbubbles.

Microbubbles have been the object of many studies owing to their multifarious applications and the ability to generate a relatively strong streaming field [37]. A recent review [9] provides a comprehensive summary of their current utilisations such as fluid pumping [34, 35], mixing [15, 14, 2, 1], selective particles trapping [27, 37, 38] and focusing [23, 38]. However, it is usually challenging generate bubbles to a specific geometry, which in turns affect its resonant frequency. The most common method to overcome this obstacle, hence maintaining a stable and prescribed bubble diamater, is "Lateral Cavity Acoustic Transducer" (LCAT) [34].

In this study, we use a modified version of LCAT that assumes the shape of a cylinder instead of a cuboid. The generated meniscus is then utilised to focus particles (2.01 and 6.60 μm), which are entering the channel at a relatively high average velocity of up to 15 mm/s, into the region opposite to the bubble. The strength of the streaming field close to the bubble surface implies the significant role shear stress plays in diverting the particles from their undisturbed streamlines. In order to understand how the induced vortices collect the particles, an analysis on the quasi-transient state is given. Finally, we investigate the effect of excitation amplitude on focusing efficiency, i.e. the focusing region's width.

Theory

When an air bubble surface is subjected to a sinusoidal acoustic field, its motion induces a first-order flow inside the oscillatory boundary layer (BL) of which the thickness is given by the equation:

$$\delta = \sqrt{\frac{2\nu}{\omega}} \tag{1}$$

where ν is the fluid's kinematic viscosity and ω is the excitation angular frequency.

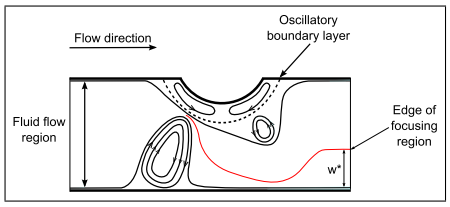

Figure 1: Schematic of fluid flow and the two vortices. w^* is the dimensionless focusing width.

This flow subsequently generates a second-order streaming field outside of the BL. For our experiments, δ is less than approximately 1.5 μm. In this BL, the shear stress is considerable due to its high velocity gradient [28] and has been theoretically studied [16]. Using the more familiar microbubbles of spherical shape, a theoretically weaker stress field than that inside the BL [4, 7] has been demonstrated to be capable of transporting particles [17, 18]. Despite the streaming behaviour being fundamentally different between a spherical and a cylindrical bubble surface [39, 25], it is reasonable to expect that a similarly strong stress field will appear in the vicinity of the latter, which can be utilised as a diversion mechanism.

In order to make use of the stress field, the incoming particles must pass a small gap between the left vortex and the boundary layer. This gap which is the result of continuity has been used for trapping of particles based on their diameters, of which the smallest trappable size D_c can be approximated by:[37, 38]

$$D_c = \frac{Q}{u_s H}, \tag{2}$$

where Q is the flowrate, u_s is the streaming velocity at the gap and H is the channel's height.

In other to describe the focusing efficiency that is applicable across different experiments, we will define a dimensionless focusing width w^* as $w^* = w/W$, where w and W is the width of the fluid region with and without particles at a particular location (i.e. when there is no actuation, $w^* = 1$ since the particles are distributed throughout the channel width). To ensure accurate measurements, both w and W are taken transversely to the flow.

Experiment setup

The microfluidic channels are fabricated using standard processes. The features are patterned onto a single side polished <100> silicon wafer by standard soft lithography techniques,

and silane (SiH_4) is deposited to render the surface hydrophobic. Polydimethylsiloxane (PDMS) (SYLGARD 184, Dow Corning®) is casted on the wafer with PDMS:curing agent 10:1 w/w. Individual channels are plasma bonded on a glass slide. A piezoelectric element (Ferroperm Piezoceramics) is adhered to a diced silicon wafer, which is also glued to the glass slide, both using epoxy resin. Figure 2 shows the 3D general shape of the air cavity. A similar design of the void has been utilised but for a completely different purpose [40]. For our devices, the channel's height and width is H = 32 μm and W = 50 μm, respectively. The gap length of the void is L = 50 μm fixed and its diameter D is either 200 or 300 μm.

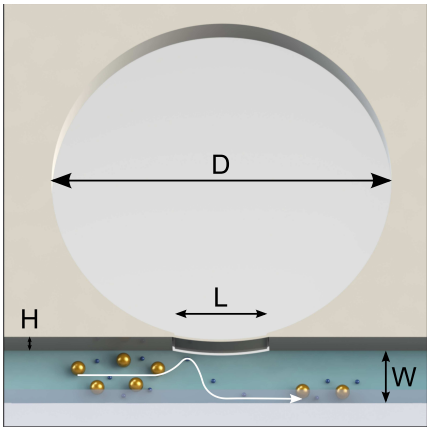

Figure 2: The sketch of the microfluidic channel. The yellow and blue spheres represent the 6.60 and 2.01 μm particles, respectively.

Polystyrene fluorescent particles of 2.01 and 6.60 μm (Bangs Laboratories, Inc.™and Magsphere, Inc. respectively) are mixed with PEG to prevent sticking on the channel's walls. The whole solution is pumped through the device by a syringe pump (kdScientific LEGATO 270). A sinusoidal signal is supplied by a signal generator (Stanford Research Systems DS345) and an amplifier (T&C Power Conversion, Inc. AG 1006).

Results and discussions

Transient analysis

To elucidate the phenomenon, we will start by analysing the transient state, here defined as the period between when the first particle is trapped in the vortex to the time the first particle is released and travels along the channel wall within the focusing region. This duration is the transient state of the focusing operation, not of the streaming itself. The time evolution of the vortex's size and brightness during this stage is shown in figure 3. When the first particle arrive, it is trapped and starts to circulate the vortex. As a result of its relatively large size, it will in fact orbit the outer rim, as shown in the first picture of part b) in figure 3. After that, other particles come in and their interactions cause them to fill the central void. The normalized intensity in part a) plot of figure 3 demonstrates this effect as it levels out after the second data point, suggesting that after the central orbit has been occupied, the subsequent particles will either follow the outer streamlines of the vortex or supersede the previous occupant of the central point. As a result, the first release of particles only occurs when the bright vortex has reached the opposite wall, indicating a "saturated" state. It should be noted that the bright vortex did not expand wider than the channel width, but rather due to the gap extruded into the air pocket at the void's corner.

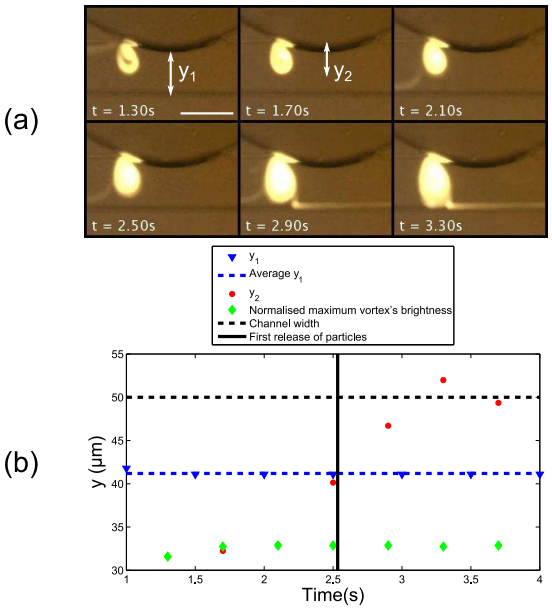

Figure 3: Transient state of vortex accumulation before the steady release of particles using 6.60 μm particles. (a) Image sequence of the vortex during the first six data points. (b) The time evolution the meniscus' location, y_1, and of size of the bright spot within the vortex while it is trapping particles, y_2, during the transient state. The scale bar represents 50 μm.

The effect of the excitation amplitude

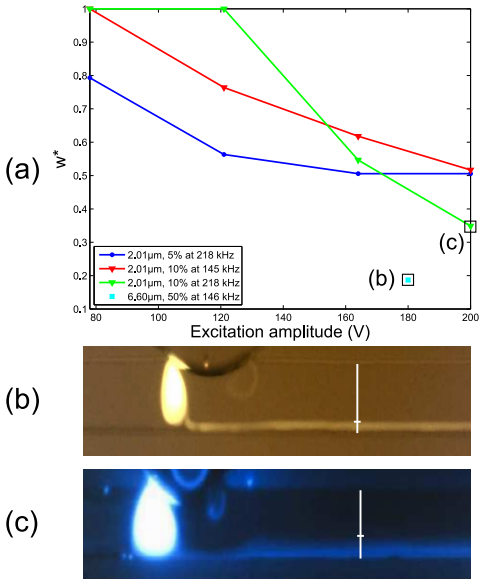

Figure 4: Focusing of 2.01 (at 5% and 10% v/v concentration) and 6.60 μm particles at 1 μL/min flowrate. (a) Focusing region as fraction of the channel width for different excitation amplitude. (b) 6.60 μm at 146 kHz and 180V are focues to approximately 0.169 of the channel (8.45 μm). (c) 2.01 μm particles at 218 kHz and 200V (10% v/v concentration) are focused to approximately 0.349 of the channel (17.45 μm). The white crosses in (b) and (c) describe how w^* is calculated.

We will now investigate the effect of varying applied voltage on the focusing width. We achieve this by changing the signal generator voltage from 0.5 to 0.8 V in 0.1 V increment while keeping the signal amplifier gain constant (this corresponds to

78 to 200 V seen by the PZT). It is expected that with weaker excitation, the oscillation amplitude of the meniscus will be increasingly dominated by the bulk flow [37, 38]. Indeed this is the case as shown in figure 4. The variations shown in figure 4(a) are due to the excitation frequency, which greatly affects the streaming field around a bubble [33].

Conclusions

In this study, we have shown that it is possible to focus particles that are uniformly entering a microfluidic channel efficiently. The device consists of a circular void that is used to trap air in order to form a bubble surface. When a sinusoidal signal is introduced, the motion of the interface induces a strong streaming field. Focusing is made possible by utilising the intense shear stress field at the bubble's boundary layer, which diverts the particles across streamlines. Experiments on 6.60 μm particles show that they can be focused to effectively a single line opposite to the meniscus. However, to characterise the physical phenomenon, we chose to analyse the empirical data based on 2.01 μm particles. The focusing process begins only when the vortex has been filled with particles. The width of the region to which particles are released decreases with increasing applied voltage, indicating better focusing. Our system is a potential candidate for pre-processing applications of cells and particles so that the resultant focusing can be utilised for different purposes.

Acknowledgements

The authors would like to thank the Australian Research Council (No. DP110104010) for their kind support of this research. This work was performed in part at the Melbourne Centre for Nanofabrication (MCN) in the Victorian Node of the Australian National Fabrication Facility (ANFF).

References

[1] Ahmed, D., Mao, X., Juluri, B. K. and Huang, T. J., A fast microfluidic mixer based on acoustically driven sidewall-trapped microbubbles, *Microfluidics and nanofluidics*, **7**, 2009, 727–731.

[2] Ahmed, D., Mao, X., Shi, J., Juluri, B. K. and Huang, T. J., A millisecond micromixer via single-bubble-based acoustic streaming, *Lab Chip*, **9**, 2009, 2738–2741.

[3] Collins, D. J., Alan, T. and Neild, A., Particle separation using virtual deterministic lateral displacement (vdld), *Lab. Chip*, **14**, 2014, 1595–1603.

[4] Collis, J., Manasseh, R., Liovic, P., Tho, P., Ooi, A., Petkovic-Duran, K. and Zhu, Y., Cavitation microstreaming and stress fields created by microbubbles, *Ultrasonics*, **50**, 2010, 273–279.

[5] Devendran, C., Gralinski, I. and Neild, A., Separation of particles using acoustic streaming and radiation forces in an open microfluidic channel, *Microfluidics and Nanofluidics*, 1–12.

[6] Di Carlo, D., Irimia, D., Tompkins, R. G. and Toner, M., Continuous inertial focusing, ordering, and separation of particles in microchannels, *Proceedings of the National Academy of Sciences*, **104**, 2007, 18892–18897.

[7] Doinikov, A. A. and Bouakaz, A., Acoustic microstreaming around a gas bubble, *The Journal of the Acoustical Society of America*, **127**, 2010, 703–709.

[8] Gralinski, I., Raymond, S., Alan, T. and Neild, A., Continuous flow ultrasonic particle trapping in a glass capillary, *J. Appl. Phys.*, **115**, 2014, 054505.

[9] Hashmi, A., Yu, G., Reilly-Collette, M., Heiman, G. and Xu, J., Oscillating bubbles: a versatile tool for lab on a chip applications, *Lab. Chip*, **12**, 2012, 4216–4227.

[10] Kamholz, A. E., Weigl, B. H., Finlayson, B. A. and Yager, P., Quantitative analysis of molecular interaction in a microfluidic channel: the t-sensor, *Anal. Chem.*, **71**, 1999, 5340–5347.

[11] Kuntaegowdanahalli, S. S., Bhagat, A. A. S., Kumar, G. and Papautsky, I., Inertial microfluidics for continuous particle separation in spiral microchannels, *Lab on a Chip*, **9**, 2009, 2973–2980.

[12] Laurell, T., Petersson, F. and Nilsson, A., Chip integrated strategies for acoustic separation and manipulation of cells and particles, *Chem. Soc. Rev.*, **36**, 2007, 492–506.

[13] Li, H., Friend, J. R. and Yeo, L. Y., Surface acoustic wave concentration of particle and bioparticle suspensions, *Biomedical microdevices*, **9**, 2007, 647–656.

[14] Liu, R. H., Lenigk, R., Druyor-Sanchez, R. L., Yang, J. and Grodzinski, P., Hybridization enhancement using cavitation microstreaming, *Anal. Chem.*, **75**, 2003, 1911–1917.

[15] Liu, R. H., Yang, J., Pindera, M. Z., Athavale, M. and Grodzinski, P., Bubble-induced acoustic micromixing, *Lab. Chip*, **2**, 2002, 151–157.

[16] Liu, X. and Wu, J., Acoustic microstreaming around an isolated encapsulated microbubble, *The Journal of the Acoustical Society of America*, **125**, 2009, 1319–1330.

[17] Marmottant, P. and Hilgenfeldt, S., A bubble-driven microfluidic transport element for bioengineering, *Proc. Natl. Acad. Sci. U. S. A.*, **101**, 2004, 9523–9527.

[18] Marmottant, P., Raven, J., Gardeniers, H., Bomer, J. and Hilgenfeldt, S., Microfluidics with ultrasound-driven bubbles, *Journal of Fluid Mechanics*, **568**, 2006, 109–118.

[19] McClain, M. A., Culbertson, C. T., Jacobson, S. C., Allbritton, N. L., Sims, C. E. and Ramsey, J. M., Microfluidic devices for the high-throughput chemical analysis of cells, *Anal. Chem.*, **75**, 2003, 5646–5655.

[20] Mitchell, P., Microfluidics-downsizing large-scale biology, *Nat. Biotechnol.*, **19**, 2001, 717–721.

[21] Morijiri, T., Sunahiro, S., Senaha, M., Yamada, M. and Seki, M., Sedimentation pinched-flow fractionation for size-and density-based particle sorting in microchannels, *Microfluidics and nanofluidics*, **11**, 2011, 105–110.

[22] Oakey, J., Applegate Jr, R. W., Arellano, E., Carlo, D. D., Graves, S. W. and Toner, M., Particle focusing in staged inertial microfluidic devices for flow cytometry, *Anal. Chem.*, **82**, 2010, 3862–3867.

[23] Patel, M. V., Tovar, A. R. and Lee, A. P., Lateral cavity acoustic transducer as an on-chip cell/particle microfluidic switch, *Lab. Chip*, **12**, 2012, 139–145.

[24] Petersson, F., Nilsson, A., Holm, C., Jonsson, H. and Laurell, T., Continuous separation of lipid particles from erythrocytes by means of laminar flow and acoustic standing wave forces, *Lab. Chip*, **5**, 2005, 20–22.

[25] Rallabandi, B., Wang, C. and Hilgenfeldt, S., Two-dimensional streaming flows driven by sessile semicylindrical microbubbles, *Journal of Fluid Mechanics*, **739**, 2014, 57–71.

[26] Rogers, P., Gralinski, I., Galtry, C. and Neild, A., Selective particle and cell clustering at air–liquid interfaces within ultrasonic microfluidic systems, *Microfluidics and nanofluidics*, **14**, 2013, 469–477.

[27] Rogers, P. and Neild, A., Selective particle trapping using an oscillating microbubble, *Lab. Chip*, **11**, 2011, 3710–3715.

[28] Rooney, J. A., Hemolysis near an ultrasonically pulsating gas bubble, *Science*, **169**, 1970, 869–871.

[29] Seo, J., Lean, M. H. and Kole, A., Membraneless microseparation by asymmetry in curvilinear laminar flows, *Journal of Chromatography A*, **1162**, 2007, 126–131.

[30] Shi, J., Huang, H., Stratton, Z., Huang, Y. and Huang, T. J., Continuous particle separation in a microfluidic channel via standing surface acoustic waves (ssaw), *Lab. Chip*, **9**, 2009, 3354–3359.

[31] Shi, J., Mao, X., Ahmed, D., Colletti, A. and Huang, T. J., Focusing microparticles in a microfluidic channel with standing surface acoustic waves (ssaw), *Lab. Chip*, **8**, 2008, 221–223.

[32] Sia, S. K. and Whitesides, G. M., Microfluidic devices fabricated in poly(dimethylsiloxane) for biological studies, *Electrophoresis*, **24**, 2003, 3563–3576.

[33] Tho, P., Manasseh, R. and Ooi, A., Cavitation microstreaming patterns in single and multiple bubble systems, *J. Fluid Mech.*, **576**, 2007, 191–233.

[34] Tovar, A. R. and Lee, A. P., Lateral cavity acoustic transducer, *Lab. Chip*, **9**, 2009, 41–43.

[35] Tovar, A. R., Patel, M. V. and Lee, A. P., Lateral air cavities for microfluidic pumping with the use of acoustic energy, *Microfluidics and Nanofluidics*, **10**, 2011, 1269–1278.

[36] Vig, A. L. and Kristensen, A., Separation enhancement in pinched flow fractionation, *Appl. Phys. Lett.*, **93**, 2008, –.

[37] Wang, C., Jalikop, S. V. and Hilgenfeldt, S., Size-sensitive sorting of microparticles through control of flow geometry, *Appl. Phys. Lett.*, **99**, 2011, 034101.

[38] Wang, C., Jalikop, S. V. and Hilgenfeldt, S., Efficient manipulation of microparticles in bubble streaming flows, *Biomicrofluidics*, **6**, 2012, 012801.

[39] Wang, C., Rallabandi, B. and Hilgenfeldt, S., Frequency dependence and frequency control of microbubble streaming flows, *Physics of Fluids (1994-present)*, **25**, 2013, 022002.

[40] Xu, Y., Lv, Y., Wang, L., Xing, W. and Cheng, J., A microfluidic device with passive air-bubble valves for real-time measurement of dose-dependent drug cytotoxicity through impedance sensing, *Biosensors and Bioelectronics*, **32**, 2012, 300–304.

[41] Yamada, M., Nakashima, M. and Seki, M., Pinched flow fractionation: continuous size separation of particles utilizing a laminar flow profile in a pinched microchannel, *Anal. Chem.*, **76**, 2004, 5465–5471.

[42] Zhang, C., Khoshmanesh, K., Mitchell, A. and Kalantar-Zadeh, K., Dielectrophoresis for manipulation of micro/nano particles in microfluidic systems, *Anal. Bioanal. Chem.*, **396**, 2010, 401–420.